Master's thesis

NTNU
Norwegian University of Science and Technology
Faculty of Natural Sciences
Department of Physics

Tord Kvernevik Sætren

Cleaning methods and aluminium growth on yttrium iron garnet

A photoemission study

Master's thesis in Master of Science in Physics
Supervisor: Justin Wells
May 2019

NTNU
Norwegian University of
Science and Technology

Tord Kvernevik Sætren

Cleaning methods and aluminium growth on yttrium iron garnet

A photoemission study

Master's thesis in Master of Science in Physics
Supervisor: Justin Wells
May 2019

Norwegian University of Science and Technology
Faculty of Natural Sciences
Department of Physics

NTNU
Kunnskap for en bedre verden

Acknowledgment

I would like to thank my supervisor's postdoctral researcher Alex Shenck. He trained me in using the lab independently. He has been helpful for bouncing ideas, getting quick feedback both during and after the project. Also for helping me learning peakfitting. I would also like to thank Håkon Røst for helping me with peakfitting. Lastly I would like to thank my supervisor for helping me having goals to work towards. His feedback has been helpful to make me refine and improve my experiments.

T.S.

Summary and Conclusions

Understanding metal thin film growth on yttrium iron garnet(YIG) is a useful step before one can studying magnon-electron interaction to bridge the gap between electronics and spintronics. Magnon-electron interaction at a metal-magnetic insulator interface can be studied using photoemission(PE), but requires a clean smooth ordered surface as well as a pure metal thin film in order to measure the effect. Aluminium has been chosen as test case for thin films on YIG in order to check if metal films react with YIG. Aluminium proved to be a material poorly suited to grow as a metal film on top of YIG because it oxidises on contact with YIG, creating a layer of aluminium oxide. YIG had no problems with charging when doing PE, despite it being an insulator. It was relatively easy to clean single crystal YIG by heating it to 400 °C in $\approx 10^{-6}$ mbar O_2 atmosphere. Even easier with the polycrystalline YIG, since it could be cleaned with fine sandpaper and a nitrogen gun. However even the single crystal YIG had a rough or disordered surface, which will create a challenge for growing ordered metal films on top. A inert metal able to relatively form a ordered surface on top is needed.

Contents

Chapter 1

Motivation and introduction

Yttrium iron garnet(YIG) is a material which has been used in spintronics to study effects such as spin pumping and spin magnetoresistance[12][19]. It is an ferrimagnetic insulator thus it has magnon transport, but no free electrons. This makes for a useful material use for studying spintronics as there are no free electrons with competing effects. In order to make spintronics compatible with modern technology it is important to bridge the gap between spintronics and electronics. Thus it is of interest to study the interface between a material with purely magnon transport(YIG) and a material with purely electron transport(metal) to study interactions between magnons and free electrons. This interaction has been reported in single crystal iron[6] using photoemission(PE), but has not been studied in a metal-ferromagnetic insulator system. First a PE study of YIG has to be done, since this has not been properly done since the 1970s[9], but also to check if it is possible to grow pure metal on YIG. The metal has to be grown as a thin film due to PE being a surface sensitive method. The film needs to be conductive Aluminium was chosen because it is a simple metal, with a band structure that have already been calculated[16]. However light metals are reactive and oxidises easily,leaving it to no longer be conductive. Aluminium is a good test case to check if light metals oxidises when introduced to YIG as it is a reactive metal.

Chapter 2

Methods and Theory

2.1 Photoemission

The main analytic tools used in this thesis are based on PE. This section will give a basic explanation of PE for readers who are not familiar with the concept. There are several books which go more in depth into PE than what is reasonable in this thesis. The main sources used for PE are two books written by Hüfner [8] and Watts [20]. The book written by Hüfner focuses more on the theory behind PE, while Watts' book has more general approach on the principles behind PE.

The main principle of PE is to measure the intensity of electrons with a specific kinetic energy. These electrons are ejected from the sample by exciting them with photons. The photons need to be energetic enough to overcome both the binding energy and the work function to emit electrons. The electrons will then be emitted with a kinetic energy given by

$$E_k = \hbar\omega - \phi_S - |E_b|, \tag{2.1}$$

were $\hbar\omega$ is the photon energy, ϕ_S is the work function of the sample and E_b is the binding energy below the Fermi level. Due to the analyser being in electrical contact with the sample, the work function of the sample is swapped out with the work function of the analyser[17]. Figure 2.1 illustrates the PE process and also gives a graphical explanation of why the work function of the sample can be omitted. Due to the electric contact, there will be a contact potential between the

analyser and sample, accelerating the electrons. The kinetic energy is then shifted by $\phi_S - \phi_A$, were ϕ_A is the work function of the analyser, allowing for (2.1) to be rewritten as

$$E_k = \hbar\omega - \phi_A - |E_b|. \tag{2.2}$$

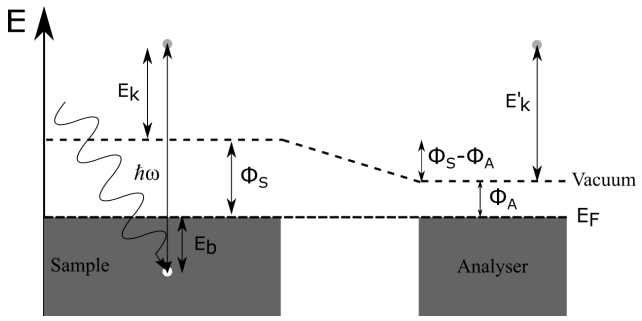

Figure 2.1: Illustration of the PE process. An electron is knocked out of the material by a photon. The kinetic energy can then be measured and used to calculate the binding energy. Due to electric contact between the sample and the analyser, the kinetic energy is changed due to a difference in the work function. The binding energy can then be calculated without any sample dependent terms.

Not all the excited electrons manage to escape the sample. On their way out they scatter both elastically and inelastically, resulting in either a attenuation of intensity or a intensity step in the spectrum at each peak. The average length an electron can travel without scattering, the mean free path is for electrons roughly a few nanometers. This means that PE is only able to probe a few nanometers into the sample i.e. the surface.

2.1.1 X-ray photoemission spectroscopy (XPS)

Every material have a discrete set of electrons with a unique binding energy, producing a set of characteristic photoelectron peaks. These discrete electrons come from the core level of the material's electronic structure, which have a high binding energy. In order to measure these electrons, they need to be excited by energetic photons, more specifically, X-rays. The intensity of emitted electrons is proportional to the number density of atoms in the sample, allowing XPS to be used as a quantitative tool. The electrons in the sample generally interacts easily resulting in shifts, broadening and generation of new peaks. A useful type of shift seen in XPS is due to different materials binding to each other. In Hüfner [8] this is explained as a change in

screening of the nucleus due to outer electrons being pulled more towards one of the materials. This effect is called chemical shift, it can be used to check which elements are bonded to each other. The values of these shifts are given in handbooks such as [1]. Another effect that can shift the peaks is charging. This can happen if the sample is not grounded or has a low enough conductance for the sample not to be able to draw electrons from ground. The sample will become positively charged and reduce the kinetic energy of the electrons. This will shift entire the spectrum to higher binding energy, since the charging is not constant in time it will smudge and shift peaks as the spectrum is measured. Another type of effect happens if the X-ray source is not monochromatic. This will broaden peaks and can also create ghost peaks. The ghost peaks are clones of the original peaks, basically it is a convolution between the X-ray spectrum and the electron spectrum. The relative size and shift of the ghost compared to the main peak is dependant on the type of material used as X-ray source and is also given in [1], this effect is simulated in Figure 2.2. Aluminium is one of several metals with an additional type of additional peaks, these peaks appear due to emitted electrons interacting with quantized oscillation of free charged particles[8], which result in an energy loss in kinetic energy. This effect is referred to as plasmon loss as the quantized oscillations are quasi-particles named plasmons. This effect will not appear in aluminium oxide since has a low free electron density. Every peak that is not from s-orbital electrons are also split in two separate peaks due to spin-orbit coupling[20], these pairs are referred to as doublets. At this point it is fitting to introduce the notation naming the peaks. It is in the form $\mathrm{X}nl_j$, were X is the atomic symbol, n is the principal quantum number, l is the orbital quantum number and j is the total angular quantum number. Sometimes the j-number is omitted from the notation both in the case of l =s or when the split is small enough for the pair to look like a single peak. The j-number gives information on the size the relative size of the doublet. The intensity ratio of the pair is equal to the degeneracy ratio, were the degeneracy is given by $2j+1$. The energy split of the doublet is unique for the element and can be found in handbooks.

2.1.2 Ultraviolet photoemission spectroscopy (UPS)

The main difference between XPS and UPS is the energy of the photons. As the name implies UPS uses ultraviolet radiation which is less energetic than X-rays. The lower energy of the pho-

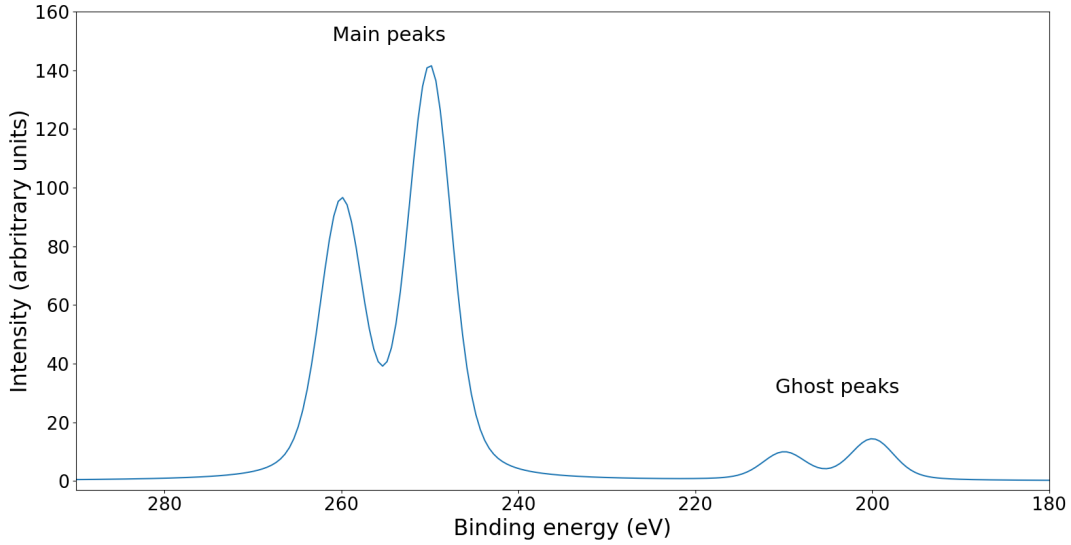

Figure 2.2: Simulation of ghost peaks. The ghosts are the two smaller peaks to the right in the figure. They are clones of the pair of peaks to the left in the spectrum. In this case the ghosts has 10% of the intensity of the main peaks and are shifted by 50 eV.

tons will not be able to excite most core levels. However they are able to excite electrons from the valence band. This will result in a energy resolved spectrum representing the valence band. The valence band is highly sensitive to doping, and thus a UPS measurement of clean single crystal YIG is useful as a reference for future projects with single crystal YIG.

2.1.3 Measuring the spectra

To measure electrons a hemispherical analyser is used. As seen in Figure 2.3 electrons enter into the lens stack of the analyser, here a potential V_{acc} is applied to retard the electrons. V_{acc} can be expressed as $V_{acc} = \frac{E_{scan}-E_{pass}}{e}$, where E_{scan} is the current energy the analyser is scanning at, E_{pass} is an user defined energy and e is the elementary charge. Electrons with $E_{kin} = E_{scan}$ will have their kinetic energy reduced to $E_{kin} = E_{pass}$ by the retarding field before they enter the hemisphere. Inside the hemisphere a potential is applied between the inner and outer hemisphere. This potential will only allow electron with kinetic energy

$$E_{kin} = e\Delta V \frac{R_1 R_2}{R_2^2 - R_1^2} \tag{2.3}$$

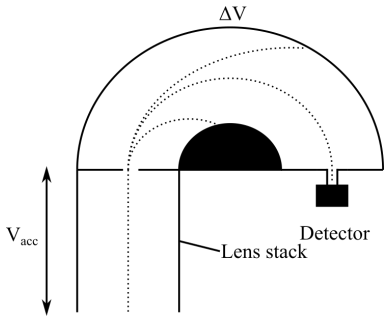

Figure 2.3: A hemispherical analyser used in photoemission. Electrons with the scanned kinetic energy is in the lens stack retarded by V_{acc} to the user defined E_{pass}. Inside the hemisphere a voltage difference ΔV applied between the inner and outer wall. This will filter out electrons which have a higher or lower energy than E_{pass}. As a final way of hinder unwanted electrons they pass through an exit slit. The slit will stop electrons with a different energy, but not electrons which enter with a slight angle.

to reach the detector, R_1 and R_2 is the radius of the inner and outer hemisphere respectively and ΔV is the tunable potential between the inner and outer wall [20]. The radial factor is constant for the analyser and is condensed to $k = \frac{R_1 R_2}{R_2^2 - R_1^2}$. Resulting in an expression for filtering out electrons with a kinetic energy different from E_{pass} by tuning ΔV to

$$\Delta V = \frac{E_{pass}}{ek}. \tag{2.4}$$

However the detector is no a perfect spot it will therefore also collect electrons which is close to E_{pass}. To further increase the energy resolution a slit is added before the detector. This will block out some of the incoming electrons, decreasing the intensity, but improving the energy resolution. This is a strongly recurring pattern in photoemission, improved resolution comes at the cost of loss in intensity. Another way of improving the resolution is to change E_{pass}. A high E_{pass} will allow a wider energy range of electrons to reach the detector, while a lower E_{pass} will have a narrower. This claim can be understood by looking at the change in radius in the circular path as the kinetic energy changes

$$\Delta r \propto \frac{\Delta E_{kin}}{E_{pass}},$$

were ΔE_{kin} is the deviation from E_{pass} and Δr is the deviation from the $E_{kin} = E_{pass}$ path. Now it is simpler to see that when E_{pass} is high, a change in E_{kin} will result in a smaller change in radius than for a low E_{pass}.

2.1.4 PE spectrum and peakfitting

To get useful results from XPS one needs to quantify the intensity of the PE peaks. This is done by fitting model peaks to the data and calculate their area. In order to get a sensible fit, one needs to have a understanding of the shape of the peaks measured. The shape of the actual PE peak is a lorentz distribution [8]. However when measuring, the X-ray source will broaden the signal in a gaussian way. This will result in a convolution of the spectrum with a gaussian [5], the resulting peak will then be a voigt function. The peak fitting for this thesis was done in Python by using the lmfit package, which had inbuilt functions for curve fitting.

2.1.5 Depth profiling

XPS can be used as a tool to analyse the depth profiling in multi-layered systems. The sample in this thesis was a 3 layered system, a model of the system is shown in Figure 2.4.

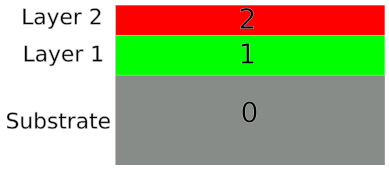

Figure 2.4: A three layered system. Each layer is indexed for making notations simpler.

For estimating the thickness of each layer a method from Ref.[11] was used. In short the method uses that the intensity from layer i is

$$I_i = n_i \sigma_i \lambda_i \left(1 - \frac{t_i}{\lambda_i}\right) e^{-\sum_{j=i+1}^{N-1} t_j/\lambda_j}, \tag{2.5}$$

were n_i is the atomic density of an element in layer i, λ_i is the energy dependant attenuation length, σ_i is the material and peak dependent photoelectron cross section, t_i is the layer thickness and N is the number of layers. The values for λ and σ_i is acquired from online databases in Ref. [3] and Ref. [2] respectively. This can then be used to get a general expression for the thickness of any layer on top of the substrate to be given as

$$t_i = \lambda_i \cdot \ln\left(\frac{I_i/(n_i\sigma_i\lambda_i)}{\sum_{j=1}^{N-1} I_j/(n_j\sigma_j\lambda_j)}\right). \tag{2.6}$$

Chapter 3

Experimental Setup

3.1 Lab

3.1.1 Ultra high vacuum(UHV)

In PE it is essential that the surfaces are as clean as possible as the method is surface sensitive. This requires techniques for both cleaning and keeping the surfaces clean. One technique to keep the sample clean is to keep it in UHV, which is a pressure lower than 10^{-8} mbar. The lower the pressure the longer the sample will stay clean. Our system uses 4 different pumps. The simplest one is the rotary pump, which is essentially a vacuum cleaner. It is able to handle large volumes of gas. The second stage is the turbo molecular pump, which is a set of fans spinning in the range of 1000 Hz to 1500 Hz depending on the pump, these pump can get hot and break down if they have to pump at high pressure. Further another type of pump is used to further lowering the pressure. The pump used is the ion pump. It ionizes the gases in the chamber and accelerates them towards a titanium plate which knocks out some of the titanium, which reacts with the gases and coats them to the wall of the chamber. The last pump which is used is a titanium sublimation pump. It works by passing current through a titanium filament, sublimating the titanium into the chamber. The titanium will then as in the ion pump react with the gases and coat them to the wall. For more information on pumps and vacuum system see Ref. [14]. Instruments and samples tend to contain gases and other contaminants they soaked up when in atmospheric pressure. This requires them to be heated in a separate chamber in

UHV to get rid of contaminants, this prosess is commonly called outgasing.

3.1.2 X-ray source

The X-ray source used in the lab is a twin anode X-ray source with both an aluminium and a magnesium anode. The X-rays are generated by bombarding the anode with electrons from a hot filament[20]. The incoming electrons excite electrons in the anode leaving holes which when filled will emit X-ray similarly to fluorescence, but with electrons instead of higher energy photons. In all the measurements presented in this thesis a magnesium anode was used. The main peak of the magnesium anode is at 1253.6 eV, the most prominent ghost peak is displaced by 8.4 eV and has 8% of the intensity.

3.2 Samples and preparation

3.2.1 Substrate

The substrate used in this project was YIG. The chemical formula of YIG is $Y_3Fe_5O_{12}$, it contains a lot of oxygen, which might get stolen by aluminium. It is a ferrimagnetic insulator with known magnon energy of ~54 meV[15]. Two versions of the sample was acquired. One of the samples were polycrystalline YIG used to study the growth. The other one was single crystal YIG which we would use to test non-destructive cleaning methods and also investigate the ordering of the surface. The orientation of the single crystal YIG was along the (111) axis. Both substrates were supplied by American Elements. The polycrystalline sample was used several times and cleaned by polishing with fine sandpaper. Organic solvents seemed to get absorbed into the sample which contaminated it further. This could still be cleaned with polishing, but a thicker layer had to be polished away after using solvent. The single crystal YIG was not cleaned by polishing since this would make the surface rough. It was instead cleaned by heating it in low pressure pure oxygen atmosphere to burn off the carbon contaminants. The reasoning behind annealing in oxygen was to make it possible to burn off the carbon contaminating the sample and also done to avoid oxygen diffusing from the sample, as this is a know problem with YIG[10].

3.2.2 Aluminium evaporator

The aluminium was grown by evaporating it in UHV directly onto the sample. There were 3 different iterations of the evaporator. The first iteration was aluminium wrapped in tantalum foil as illustrated and shown in Figure 3.1. This design was not suitable to evaporate aluminium as the two metals started alloying before any aluminium would be evaporated onto the sample. This tantalum-aluminium alloy had a higher evaporation temperature than pure aluminium and would not evaporate any pure aluminium at a reasonable temperature i.e. below 1500 °C.

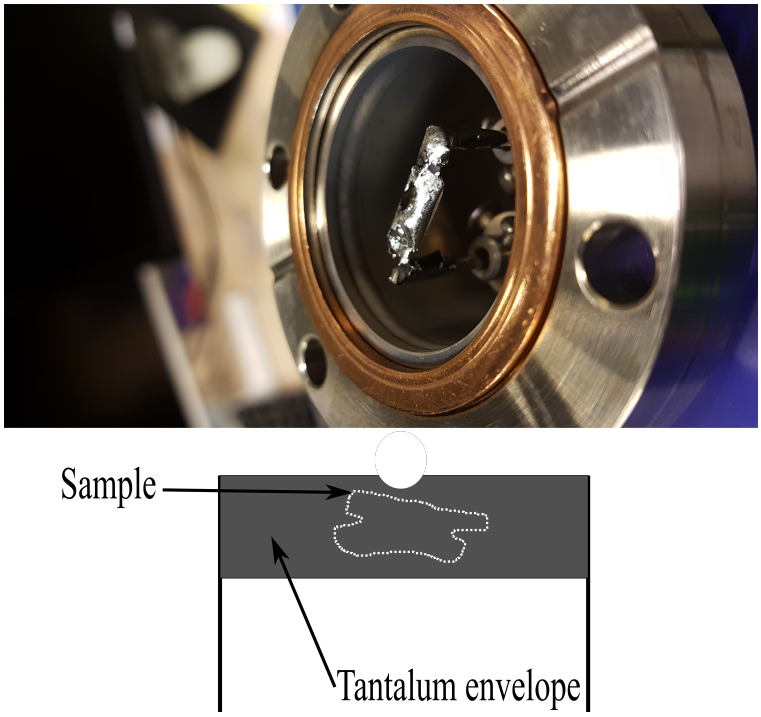

Figure 3.1: The tantalum foil design for the aluminium evaporator. Aluminium and tantalum alloyed resulting in holes in the foil as the aluminium was dissolving it, until the circuit broke.

The second iteration was a crucible made of scrap Al_2O_3 ceramic tube wrapped in 0.38 mm thick tungsten wire it seen in Figure 3.2. This design showed some promise, but had some drawbacks. The 1 mm walls of the ceramic tube was a bit thick, this required a lot of heating to heat the pure aluminium inside. The high temperature also made water cooling of the chamber essential to avoid structural damage, users accidentally burning themselves or to avoid outgasing the chamber, which would contaminate the sample. Also it seemed that the ceramic released oxygen when heated, resulting in growing aluminium oxide instead of pure aluminium, this is discussed more thoroughly in the results section.

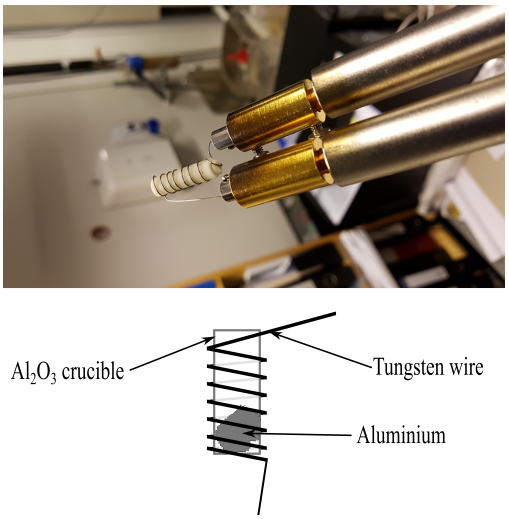

Figure 3.2: The crucible made for the second iteration of the aluminium evaporator. The walls of the crucible was too thick heat the aluminium without damaging the crucible. Unlike the other designs this is reusable.

The final iteration was a tungsten coil filled with a small chunk of aluminium, made with the same thickness wire as in the crucible design. The aluminium would melt and stick to the wire forming a coating which could be evaporated. This evaporator needed little materials and was thus much quicker to degas. Like with the tantalum foil the aluminium also alloyed with the tungsten wire. However it seemed to alloy slower with the wire than with the foil, slow enough for it to be able to grow aluminium. The growth rate did deteriorate after some uses due to the alloying. The alloying would also make it brittle, in Figure 3.3 the coil design is shown, before and after use, as well as a illustration of the design.

3.2.3 Gold evaporator

The design used to grow gold onto silicon was the same as in the first iteration of the aluminium evaporator. A small gold wire wrapped in a thin tantalum foil. This design managed to grow a gold film without any oxygen contamination, making a film suitable for testing the evaporator.

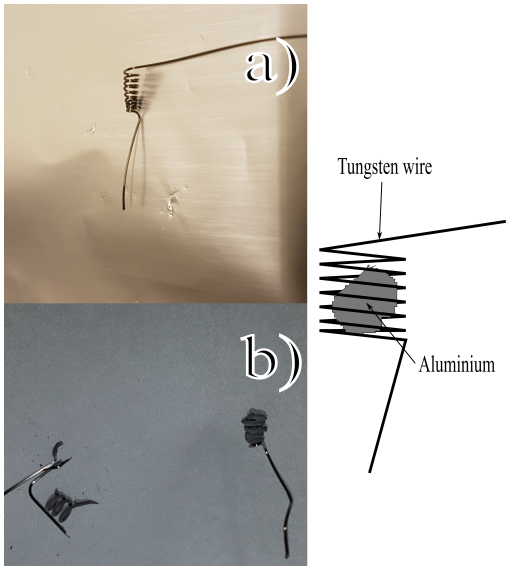

Figure 3.3: **a)** Coil design used for the final iteration of an aluminium evaporator. Grows clean aluminium, but the growth rate deteriorates after some uses due to alloying. **b)** The alloying between the coil and the aluminium made the coil extremely brittle. This was not able to grow aluminium as any more aluminium introduced would alloy quickly.

Chapter 4

Results and discussion

4.1 Efficiency of cleaning methods

The cleanliness of the sample was checked by doing a widescan of the sample and check for peaks from elements that was not expected. The widescan of the polycrystaline and single crystal YIG before and after cleaning is plotted in Figure 4.1 and Figure 4.2 respectively. From the widescans one can see that in general the polycrystaline YIG has more carbon contaminants than the single crystal YIG. The cleanlines is quantified by simply comparing the height ratio carbon peak to largest yttrium peak. The as loaded polycrystaline YIG more carbon with a ratio of 6.74, while the single crystyal YIG had a ratio of 0.83 before cleaning. The main reason the polycrystaline YIG was more contaminated is most likely due to an attempt to clean it in ethanol. Polishing it with sandpaper did manage to reduce the ratio to 0.27, this also required using a nitrogen air gun to blow off the loose powder left after polishing it. However cleaning the single crystal YIG by heating it got the ratio down to 0.11, by far the method that got the cleanest sample.

4.2 UPS and Low energy electron diffraction(LEED)

In Figure 4.3 the UPS data of the single crystal YIG is presented. As seen in the figure the spectrum is more intense than XPS spectrum, in order to avoid damaging the analyser a smaller slit was used as high intensity can burn the detector. The quality if the data was good enough to

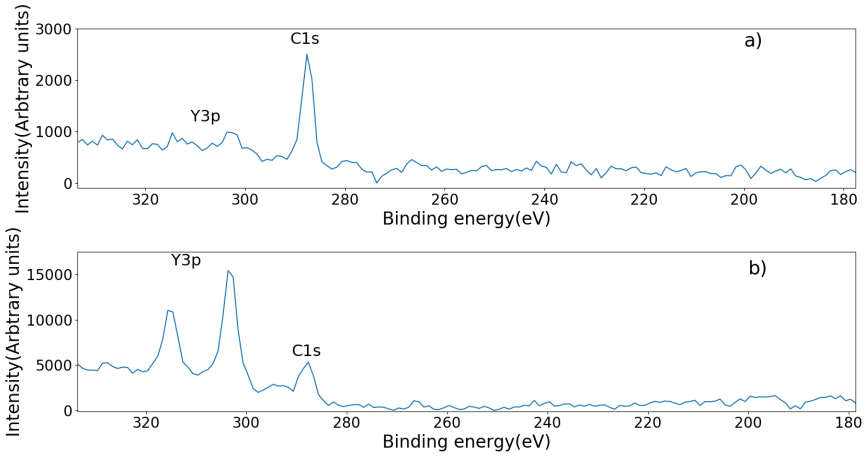

Figure 4.1: Before and after cleaning the polycrystaline YIG. **a)** Polycrystaline YIG before cleaning. Due to bad handling the sample it was highly contaminated drowning out most of the signal from the actual sample.**b)** Polycrystaline YIG after cleaning with sandpaper. This method of cleaning was also able to clean off aluminium after evaporation.

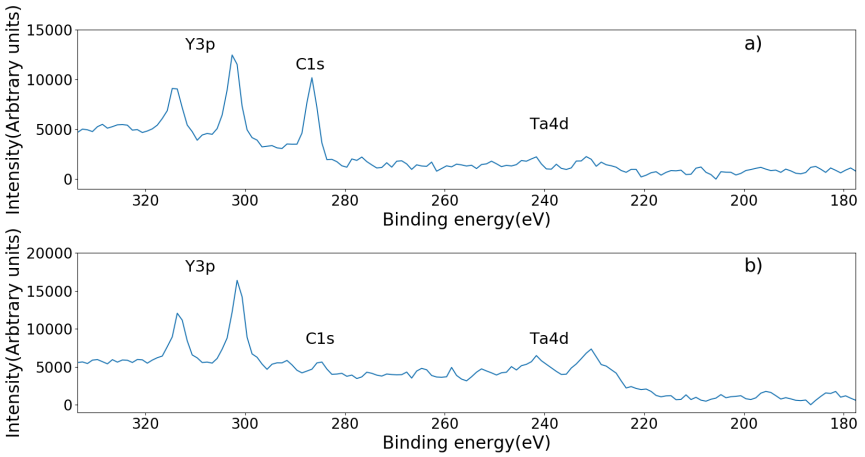

Figure 4.2: Before and after cleaning the single crystal YIG. **a)** Single crystal YIG before cleaning. A prominent carbon peak can is in the all though less than the polycrystaline sample. The small doublet of tantalum can also be seen, this is from the x-ray beam also hitting the tantalum clamps that keep the sample in place. **b)** Single crystal YIG cleaned by heating. This method was slower than sandpaper, but not as destructive on the surface.

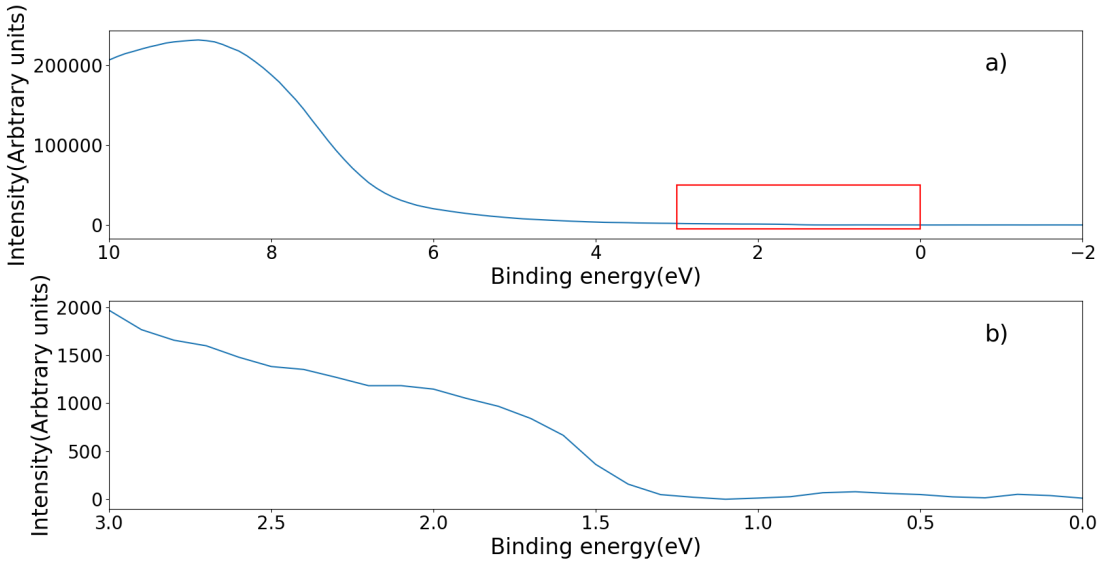

Figure 4.3: **a)** UPS of the single crystal YIG. The UPS spectrum is more intense than the XPS, supporting that the sample do not have charging problems. **b)** The same spectrum, but zoomed in on the top of the valence band. The quality of the data further supports that YIG do not have problems with charging.

be quite certain that the sample had no problems with charging. LEED was attempted on the single crystal YIG, but no diffraction pattern appeared. The technique needs a well ordered surface in order to get a pattern[18]. That no pattern was possible to be acquired suggests that the surface of the sample is rough. It could be that the heating made the surface rough, this needs to be checked with imaging methods such as electron microscopy to see if there are any clear changes.

4.3 Aluminium evaporator quality

The XPS spectrum of the aluminium grown on gold is presented in Figure 4.5. The gold layer had no oxygen before aluminium was grown on it using the crucible design. This was a clear proof that the crucible design released oxygen. The most likely source of oxygen is the tungsten wire burning away some of the ceramic aluminium oxide as seen in Figure 4.4. Since this happened every time the evaporator was used it implied that the pure aluminium inside was not sufficiently heated. A likely reason could be that the walls of the crucible being to thick.

Figure 4.4: Burnt out crucible. The tungsten wire has clearly burnt itself into the ceramics, this is suspected to be the source of oxygen when evaporating.

Since the crucible contains aluminium as well it could also be that it is the source of aluminium, unfortunately this is difficult to verify. After growing more aluminium on using the coil design the oxygen peak became more suppressed, this is a strong indication that pure aluminium has been deposited. Another indication that pure aluminium had been deposited by the coil design is the appearance of plasmon satellites to the left of the Al2s peak, as these do not appear in aluminium oxide[4]. Considering that no spectra acquired of aluminium grown with the crucible design showed any signs of plasmons no matter how thick the layers were indicates that the crucible design is unable to produce pure aluminium, while the coil design produces aluminium clean enough for plasmons to appear. However the aluminium grown using the coil design should also have been grown on top of pure gold to give a definitive and simpler conclusion on how pure the coil grown aluminium is.

4.4 Aluminium growth on YIG

Analysis of the aluminium growth was done by doing a high resolution scan of the core levels of aluminium and yttrium. The data presented in Figure 4.6 is from a layer of aluminium grown on top of the polycrystaline sample using the crucible design. By using the method for calculating the layer depth as explained in Section 2.1.5 it was calculated that the thickness of the aluminium oxide and pure aluminium layers were 2.52 nm and 0.8 nm respectively.

The spectrum acquired for the aluminium grown with the coil design can be seen in Figure 4.7. At first glance it seems like it is even more aluminium oxide after growing with the coil

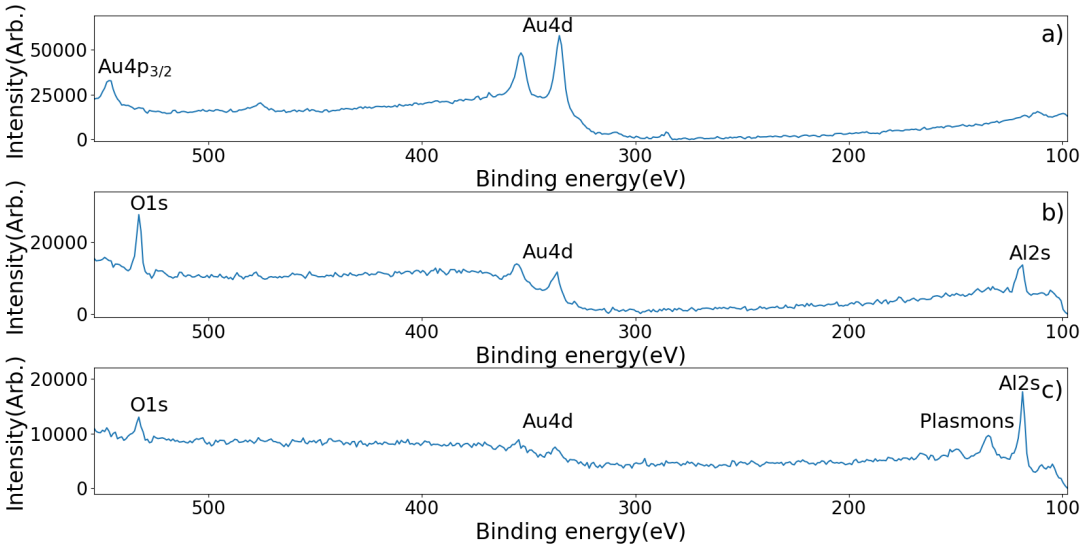

Figure 4.5: Widescan of a thick gold film grown on silicon used to test the cleanliness of the evaporators. **a)** Pure gold surface used as a reference when growing aluminium. **b)** Aluminium grown with the crucible design. The crucible grew aluminium oxide instead of pure aluminium. **c)** More aluminium grown with the coil design. The aluminium is grown on top of the aluminium oxide and not pure gold.

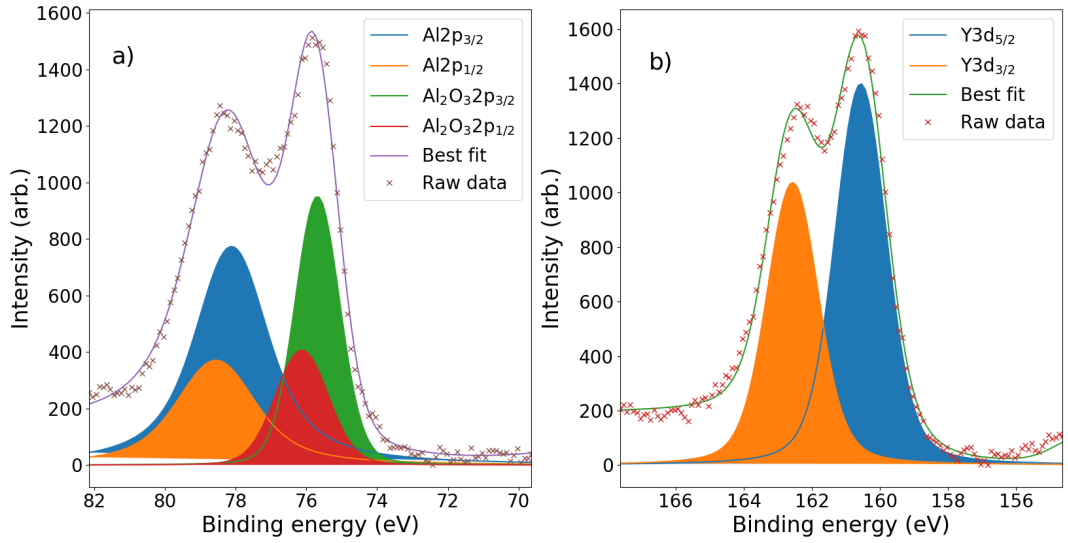

Figure 4.6: XPS spectra for aluminium grown with the crucible design. a) The Alp2 core level, the peak is split into several smaller peaks. The most important split is due to the chemical shift, this is used to differentiate the aluminium oxide and pure aluminium layers. These two peaks are further split due to spin orbit splitting. b) Y3d core level from the YIG substrate, the spin orbit split is strong enough to such make two distinct peaks.

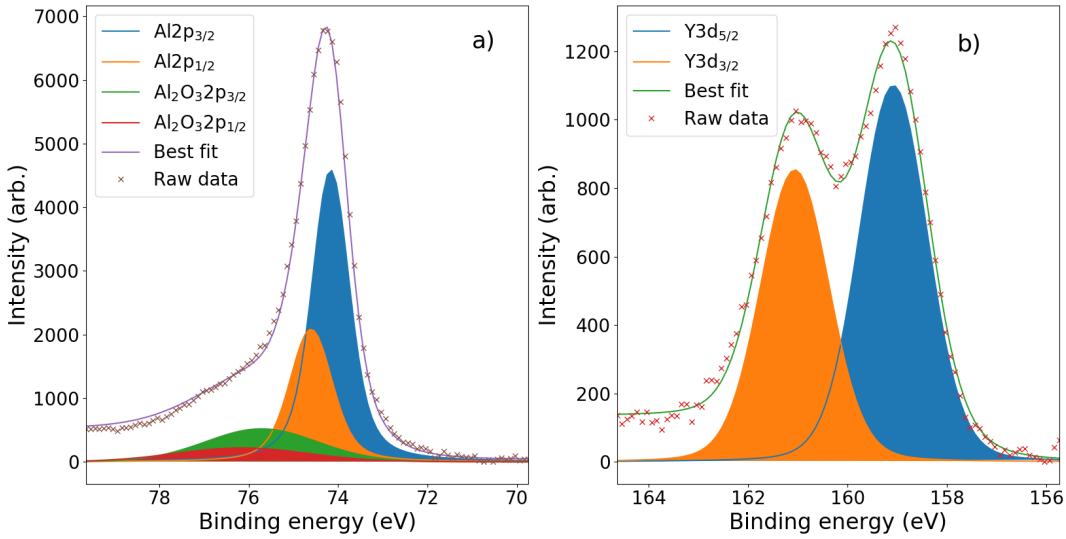

Figure 4.7: XPS spectra for aluminium grown with the crucible design a) The Alp2 core level, the peak is split into several smaller peaks. The most important split is due to the chemical shift, this is used to differentiate the aluminium oxide and pure aluminium layers. These two peaks are further split due to spin orbit splitting. b) Y3d core level from the YIG substrate, the spin orbit split is strong enough to such make two distinct peaks.

design. After closer analysis it is calculated that the oxide layer is 2.70 nm thick and the pure aluminium layer is 2.23 nm thick. The thickness of the pure aluminium is 83% of the thickness of the aluminium oxide. In the case of the crucible design the pure aluminium was 32% of the aluminium oxide layer, significantly less pure aluminium than with the coil design. However there is still a significant amount of aluminium oxide even with the coil design, indicating that the aluminium draws oxygen from YIG, making it impossible to grow metallic aluminium on top of YIG. It seems reasonable for this to happen as YIG has a high oxygen diffusion[10]. The position of the peaks are not the same for the spectrum for the different samples. This seemed to be a problem on the analyser end since the spectrum would get shifted even on the same sample if the measurement was redone a few days later. However the chemical shift between the pure aluminium peak and the aluminium oxide peaks changes between the two samples. In the case of the crucible design the chemical shift was 2.4 eV, while for the coil design it was 1.5 eV. However when comparing the oxidised peak shift with database values[13], one can see these peaks tend to have quite a large variation which often are dependant on different species

of aluminium oxide.

Chapter 5

Conclusion and further work

Several conclusions can be drawn from the results. The main conclusion that can be drawn is that aluminium is not a suitable material to use at a metal thin film on top of YIG. Due to it oxidizing by drawing oxygen from the YIG. Noble metals could be used, preferably one that can form an ordered layer on top of a substrate poorly ordered substrate, but noble metals have a more complicated band structure which could complicate the detection of electron-magnon interaction. Despite YIG being a insulator it seems not to have any charging problems. YIG is relatively simple to clean by heating it up to 400 °C in $\approx 10^{-6}$ mbar O_2 atmosphere. The lack of any LEED pattern suggests that the surface of the singe crystal YIG is rough, which might be a problem when it comes to growing a well ordered metal on top. A possible alternative substrate could be nickel oxide which is reported to have magnons with energy up to 120 meV[7], which should be simpler to see with poor energy resolution. Since nickel oxide is less complicated than YIG it could be grown in situ.

Bibliography

[1] Handbook of x-ray photoelectron spectroscopy : a reference book of standard data for use in x-ray photoelectron spectroscopy, 1992.

[2] Atomic calculation of photoionization cross-sections and asymmetry parameters, 1993. URL `https://vuo.elettra.eu/services/elements/WebElements.html`.

[3] Nist electron inelastic-mean-free-path, 1999. URL `https://www.nist.gov/srd/nist-standard-reference-database-71`.

[4] A. Barrie. X-ray photoelectron spectra of aluminium and oxidised aluminium. *Chemical Physics Letters*, 19(1):109–113, 1973.

[5] C. Battistoni, G. Mattogno, and G. Righini. Internal analyser inelastic scattering effects in xps quantitative analysis. *Surface and interface analysis*, 22(1-12):98–102, 1994.

[6] X. Cui, K. Shimada, M. Hoesch, Y. Sakisaka, H. Kato, Y. Aiura, S. Negishi, M. Higashiguchi, Y. Miura, H. Namatame, et al. High-resolution angle-resolved photoemission spectroscopy of iron: A study of the self-energy. *Journal of Magnetism and Magnetic Materials*, 310(2): 1617–1619, 2007.

[7] M. T. Hutchings and E. Samuelsen. Measurement of spin-wave dispersion in nio by inelastic neutron scattering and its relation to magnetic properties. *Physical Review B*, 6(9):3447, 1972.

[8] S. Hüfner. *Photoelectron spectroscopy : principles and applications*. Advanced texts in physics. Springer, Berlin, 3rd rev. and enl. ed. edition, 2003. ISBN 3540418024.

[9] P. Larsen, R. Metselaar, and B. Feuerbacher. Uv photoemission studies of yttrium iron garnet. In *AIP Conference Proceedings*, volume 29, pages 668–669. AIP, 1976.

[10] R. LeCraw, E. Gyorgy, R. Pierce, J. Nielsen, S. Blank, D. Miller, and R. Wolfe. Rapid oxygen diffusion in ca-doped yttrium iron garnet films at 25 to 250° c. *Applied Physics Letters*, 31 (4):243–244, 1977.

[11] A. V. Lubenchenko, A. A. Batrakov, A. B. Pavolotsky, O. I. Lubenchenko, and D. A. Ivanov. Xps study of multilayer multicomponent films. *Applied Surface Science*, 427:711 – 721, 2018. ISSN 0169-4332. doi: https://doi.org/10.1016/j.apsusc.2017.07.256. URL `http://www.sciencedirect.com/science/article/pii/S0169433217322560`.

[12] S. Manuilov, C. Du, R. Adur, H. Wang, V. Bhallamudi, F. Yang, and P. C. Hammel. Spin pumping from spinwaves in thin film yig. *Applied Physics Letters*, 107(4):042405, 2015.

[13] A. Naumkin, A. Kraut-Vass, S. Gaarenstroom, and C. Powell. Nist x-ray photoelectron spectroscopy database, 2012. URL `https://srdata.nist.gov/xps/Default.aspx`.

[14] K. Oura, V. Lifshits, A. Saranin, A. Zotov, and M. Katayama. *Surface science: an introduction*. Springer Science & Business Media, 2013.

[15] J. S. Plant. Spinwave dispersion curves for yttrium iron garnet. *Journal of Physics C: Solid State Physics*, 10(23):4805, 1977. URL `http://stacks.iop.org/0022-3719/10/i=23/a=014`.

[16] M. Read. Surface electronic band structure of aluminium (111).

[17] R. Schlaf. Calibration of photoemission spectra and work function determination. URL `http://rsl.eng.usf.edu/Documents/Tutorials/PEScalibration.pdf`.

[18] M. A. Vanhove, W. H. Weinberg, and C.-M. Chan. *Low-energy electron diffraction: experiment, theory and surface structure determination*, volume 6. Springer Science & Business Media, 2012.

[19] S. Vélez, A. Bedoya-Pinto, W. Yan, L. E. Hueso, and F. Casanova. Competing effects at pt/yig interfaces: Spin hall magnetoresistance, magnon excitations, and magnetic frustration. *Physical Review B*, 94(17):174405, 2016.

[20] J. F. Watts. *An introduction to surface analysis by XPS and AES*. Wiley, Chichester, 2003. ISBN 0470847123.

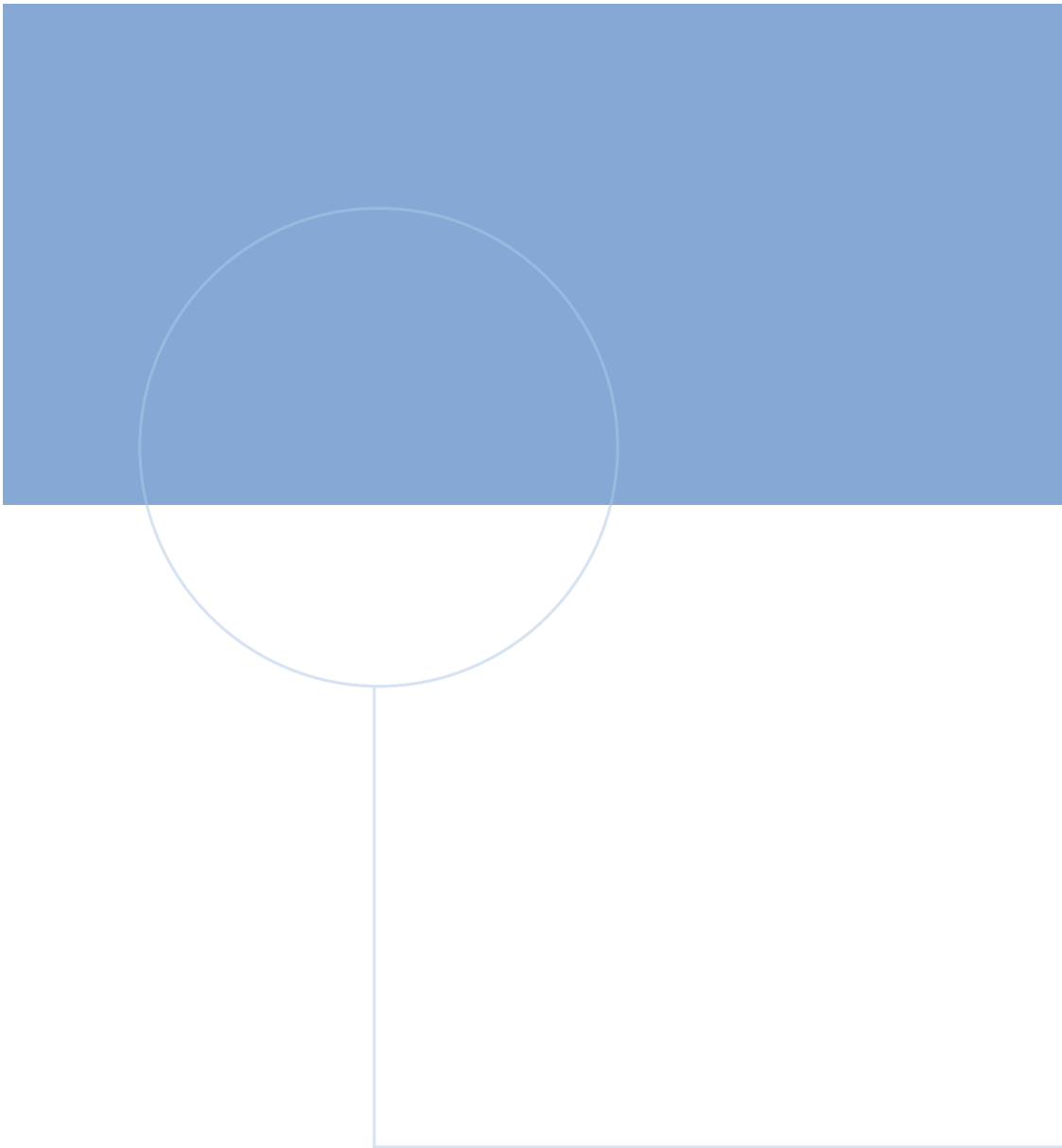

NTNU
Norwegian University of
Science and Technology